A core-shell synthesis of CaCu3Ti4O12 (CCTO) ceramics showing colossal permittivity and low electric losses for application in capacitors

Sonia de Almeida-Didry, Samir Merad, Cécile Autret-Lambert, Meledje Martin Nomel, Anthony Lucas, François Gervais

A Core-shell synthesis of $CaCu_3Ti_4O_{12}$ (CCTO) ceramics showing colossal permittivity and low electric losses for application in capacitors

Sonia De Almeida-Didry,[a] Samir Merad ~~Meradi~~,[a] Cécile Autret-Lambert,*[a] Meledje Martin Nomel,[a] Anthony Lucas,[b] François Gervais[a]

a GREMAN, UMR 7347 University of Tours François Rabelais/CNRS, Faculty of Sciences and Techniques, Parc de Grandmont, 37200 Tours, France

b SRT Microcéramique, Rue Mons, 41100, Vendôme, France

Abstract

A core-shell synthesis is applied to $CaCu_3Ti_4O_{12}$, a material that shows colossal permittivity. The objective was to test several bulk permittivity of the shell material in order to reach a large capacity of the grain boundaries after sintering. The permittivity is improved with certain shells while the bulk resistivity reaches levels approaching that of commercial grain boundary barrier layer (GBBL) ceramic capacitors. The highest permittivity is confirmed to be related to the highest capacity of grain boundaries. The bulk resistivity is related to that of grain boundaries. If one attaches the more important weight to a high bulk resistivity without need of permittivity larger than 15,000, as in commercial GBBL ceramic capacitors, several samples appear convenient. On the other hand, much higher permittivity can be reached like in CCTO with a shell of TiO_2 but at the expense of dielectric losses, possibly due to oxygen departure from stoichiometry. Thermal post-treatment under various controlled atmosphere have been applied to reduce dielectric losses.

Keywords: colossal permittivity, core-shell, Internal barrier layer capacitance, CCTO, ceramic capacitor

* Corresponding author. E-mail address: cecile.autret@univ-tours.fr

1. Introduction

The demand for electric vehicles and other technological applications implies an enhanced demand for ceramic capacitors. In addition to capacitors already on the market, promising

trends has supported the research on ceramics showing giant or colossal permittivity [1]. One extensively studies candidate is $CaCu_3Ti_4O_{12}$ [2-10]. Since pioneer works, the search on keywords ($CaCu_3Ti_4O_{12}$ OR CCTO) in the Web of Science returns more than 1700 papers published in peer-reviewed literature (Figure 1). The permittivity of studied samples currently ranges from 10^4 to 10^5, what constitutes a successful achievement. However, the dielectric losses are generally larger than 2.5 %, which is considered as the upper threshold for commercial capacitors.

The origin of the colossal permittivity has been much debated in the literature. Most recent studies tend to arrive to a consensus that the properties have their origin in the *microstructure* of the ceramics itself. Like in Grain Boundary Barrier Layer (GBBL) similar theory [1], semiconducting grains would play the role of electrodes of the capacitor while grain boundaries carry the permittivity of the capacitor [11]. The system would then consist of as many capacitors in series as the number of grains that pave a line, or a wall of bricks, along the thickness of the sample. Provided that semiconductor grains are conducting enough, the permittivity of the sample may be approximated by [1, 12, 13]

$$\varepsilon = \varepsilon_{gb} A/t \qquad (1)$$

ε_{gb} is the permittivity of the *grain boundary*, A is the size of the grain and t is the thickness of the grain boundary. If this Internal Barrier Layer Capacitance (IBLC) model [5] is applicable, the research, therefore, has to be focused not only on grains which has already been extensively studied in the literature, but more importantly on grain boundaries which, by contrast, have been somewhat less studied. Provided they are conducting enough, grains indeed do not play any role in Eq. (1) other than their size A.

A comparison of an undoped CCTO sample sintered 24 hours at 1050°C with a commercial GBBL capacitor has shown that the permittivity of the CCTO sample is currently 4 times higher (Table 1). Electric losses, however, measured via $tan(\delta) = 0.05$ at 1 kHz are still a bit too high. As a result, the sample resistivity of 1.3 10^7 should be increased for industrial applications in terms of ceramic capacitors. The microscopic reason is the following. The capacitance C_{gb} of the grain boundary reaches 4.5 10^{-7} F.cm^{-1} compared to only 10^{-10} F.cm^{-1} for the commercial GBBL capacitor. This explains the larger permittivity of CCTO via Eq. (1) rewritten

$$\varepsilon \sim C_{gb} \qquad (2)$$

since $C_{gb} \sim \varepsilon_{gb}/t$. Conversely, the resistivity R_{gb} of the grain boundary of the GBBL commercial capacitor reaches 10^{10} Ω.cm whereas that of CCTO does not exceed 8.5 10^{6} Ω.cm, focusing on the improvement which is needed.

Interesting results in terms of performance of grain boundaries and, therefore, in terms of both high permittivity and high resistivity, have been found when the grain boundary was TiO_2 of crystal structure anatase, as probed by Raman scattering [14]. Anatase indeed is a good insulator. The mechanism by which such grain boundaries were formed during the sintering process, however, is unclear and not yet controlled.

How to control the grain boundaries of CCTO to enhance their resistivity? One way which has been little exploited about CCTO up to now is the core-shell approach. The grains of CCTO are embedded in a shell of an insulating ceramic and then sintered with the hypothesis that the chosen shell will become the grain boundary. Several shell materials and several core-shell processes have been experimented in this study. The purpose is to check which one gives the highest permittivity associated with the highest resistivity.

2. Experimental

The CCTO grains have been synthesized by mixing stoichiometric amounts of $CaCO_3$, CuO and TiO_2 powders via ball-milling media in ethanol during 24 h. The resulted mixing has to be calcined at 950 °C for 24 h. The average size of CCTO particles can be evaluated by a Malvern zetasizer using dynamic light scattering. Typical value is about one micrometer. For comparison, the CCTO powder was also functionalized by PVP or by PEG. To functionalize CCTO, the powder was dispersed in ethanol and then 10 %wt of PVP or PEG was added and mixed during 24h. Using an ultrasonic bath, the synthesis of core-shell noted CCTO@Al_2O_3 [15] was promoted by sol-gel reaction. The amount of aluminum isopropoxide precursor solution (0.15 g of aluminum isopropoxide dissolved in 45 milliliters of ethanol) was calculated from the average size of CCTO particles to obtain an alumina nanocoating of 20 nanometers. Then, 5 grams of CCTO or CCTO-PVP or CCTO-PEG powder was dispersed in 420 milliliters of ethanol which has to be added in the precursor solution. It is then sonificated during 20 minutes. 50 mL of H_2O/ethanol mixture (1:5 (v/v)) has to be added. In this case, the final mixture is ultrasonicated during 2 hours. Also, the CCTO@SiO_2 core-shell was synthesized from CCTO particles by a Stöber modified process. SiO_2 has the advantage to be

insulating, which is important for a capacitor by avoiding electric leakage. It also shows a good conformal shell around the core. The thickness of the shell in addition may be easily controlled. The CCTO powder was firstly dispersed in a mixed solution of ethanol/H_2O/ammonia (75/23.5/1.5 %vol). The solution was agitated at room temperature during one hour. Then tetraethyl orthosilicate (TEOS) was added slowly under magnetic stirring. The amount of TEOS was calculated from the average size CCTO particles (~1 µm) to obtain a silica nanocoating of 20 nm. The sol-gel technique was also used to synthesize CCTO@TiO_2 core-shell. The CCTO particles was firstly mixed with absolute ethanol and the solution was placed in iced bath. Then, the titanium butoxide (TBOT) was added and the solution was mixed during 20 minutes under vigorous stirring. Secondly, a mixed solution of ethanol/H_2O/ammonia (75/23.5/1.5 %vol) was added to the first one and the resulted solution was agitated during 4 hours.

All the as-formed based CCTO core-shell powder are collected by centrifugation (305 RCF-5min). The nanocoating powder has to be washed several times with ethanol and dried overnight at 60°C.

After the collection of the CCTO@SiO_2 core-shell powder, a double core-shell of SiO_2 and Al_2O_3 noted CCTO@SiO_2@Al_2O_3 was synthesized. The same process of CCTO@Al_2O_3 was done but in the beginning instead of using CCTO, the CCTO@SiO_2 powder was dispersed.

All the pellets are then sintered at 1050°C during 5 h expect for the CCTO@TiO_2 pellet which is sintered during 24 h. A post-annealing treatment under oxygen atmosphere was realized on CCTO@Al_2O_3 pellet at 500°C during 12 h.

The sintered pellets have been analyzed using X-ray diffraction (Bruker D8) with Cu Kα a radiation of wavelength ~ 1.5418 Å. The dielectric and complex impedance data were measured in a frequency range from 100 Hz to 10 MHz at ambient temperature using an Agilent 4294A impedance analyzer. The data were fitted with the RC element model and the four parameters R_g, C_g, R_{gb}, C_{gb} were extracted as shown in more details by De Almeida-Didry *et al.* [16].

Results and discussion

An example of fit of a two RC elements model, one for the grains and one for the grain boundaries, to experimental data of CCTO@TiO_2 is shown in Figure 2. Two distinct semi-circles are expected, each being associated with a distinct dielectric process, one corresponding to ceramic grains (observed at high frequencies) and the other to grain boundaries. The permittivity and loss tangent of this core-shell sample compared to undoped CCTO and to a commercial GBBL capacitor manufactured by Johansen is shown in Figure 3. Results for each studied sample have been similarly fitted with two RC elements. The dielectric behavior of CCTO ceramics has a Debye-like relaxation with a steep decrease in dielectric constant at the frequency where the dielectric loss tangent displays a relaxation peak. The Debye-like relaxation can be explained by the Maxwell–Wagner relaxation at the interfaces between the grains and their boundaries [17-20]. Results for the grain boundaries which are of main interest in this study are reported in Table 1. Results for the grains are less accurate since the profiles of Figure 2 are mainly related to grain boundaries.

CCTO@TiO_2

The highest permittivity, 870,000, is found for the sample CCTO@TiO_2. Figure 4 compares the XRD diagram of undoped CCTO with that of a sample of CCTO@TiO_2. Additional peaks which are characteristic of TiO_2 crystalized with the rutile crystal structure are displayed in the latest samples. Table 1 shows that this highest permittivity is related to the highest C_{gb}. Among all the shells experimented in this study, rutile single crystal shows the highest permittivity averaged over the three main axes of $(\varepsilon_{//} + 2\ \varepsilon_{\perp})/3 = 108$ [21]. Rutile single crystal treated under reducing atmosphere becomes conductor [22]. It is possible, therefore, that the rutile grain boundary would have become slightly conducting, what would explain the lowest R_{gb} found among all studied samples in Table 1. As a result, the bulk resistivity of the sample is also the lowest among all studied samples.

CCTO@SiO_2

An oxide which remains a good insulator independently of thermal treatments contrary to TiO_2 is SiO_2. As a result, it has been used as the dielectric material of capacitors integrated to silicon chips for decades. It has also been used as a gate of transistors for decades. Several thicknesses of SiO_2 shells have been experimented. Best results are reported in Table 1. The resistivity, $tan(\delta)$ and R_{gb} unfortunately are not improved with respect to undoped CCTO. The permittivity is even found lower. Table 1 shows that this is related to the C_{gb} which is found 10 times lower than that of undoped CCTO. This is presumably related to the low permittivity, only 4, of bulk SiO_2.

CCTO@Al_2O_3

Table 1 shows that the sample CCTO@Al_2O_3 shows a higher permittivity than undoped CCTO while the bulk resistivity is slightly improved. No parameter appears obviously responsible for this improvement. Conversely, considerable improvement is found to be obtained by the procedure of functionalization. With PolyEthyleneGlycol (PEG), the permittivity reaches 130,000 without significant losses measured via $tan(\delta)$. In addition, the bulk resistivity is multiplied by 3 with respect to undoped CCTO. The bulk resistivity is even multiplied by 15 with respect to undoped CCTO with the functionalization by PolyVinylPyrrolidone (PVP), while the permittivity is found 27 % higher than that of undoped CCTO. The mechanisms which allowed such progresses have to be further studied. The functionalization favors the conformal shell. Since the organic species disappeared during the sintering process, the effect is assumed to be mechanical.

A post-annealing of core-shell samples under oxygen at 500°C during 12 hours increases the bulk resistivity up to 1.9 GΩ.cm, a value that becomes comparable with that of a commercial GBBL capacitor (Table 1). The permittivity however appears reduced with respect to that of the non-post-annealed sample. It still amounts to 17,000, a value higher than for the GBBL capacitor. The drop of permittivity is related to the drop of C_{gb} in Table 1.

CCTO@SiO_2@Al_2O_3

The core-shell microstructure of CCTO@SiO_2@Al_2O_3 observed by TEM is shown in Figure 5. Both distinct shells of SiO_2 and Al_2O_3 are observed in the picture. After sintering, the bulk

resistivity reaches 5 10^9 Ω.cm, not far from the 10^{10} Ω.cm of the Johanson GBBL capacitor. The permittivity nevertheless appears 11 % higher, ranking this double shell and associated process as a good challenger of GBBL capacitors.

CCTO@SiO_2@TiO_2

It was tempting to check whether a double shell combining good insulator like SiO_2 and an oxide showing a large bulk permittivity like TiO_2 rutile would improve the properties. The resistivity reaches 5.2 10^8 Ω.cm, but this is not the best result of the studied series of table 1. In addition, the permittivity is found poor. Compared to the other samples of the series, the microstructure is heterogeneous and shows SiO_2 aggregates as observed in the figure 6 that can explain the disappointing results. Grains are also smaller, what is a disadvantage in Eq. 1.

Conclusion

The core-shell approach applied to CCTO is shown to give results that compares favorably with commercial GBBL capacitor. The permittivity is improved while the bulk resistivity reaches levels comparable to commercial ceramic capacitors. The highest permittivity values are confirmed to be related to the high capacity of grain boundaries. The bulk resistivity is related to that of grain boundaries. This study shows that one may play with the bulk permittivity of the shell to try to reach large C_{gb}. However the possible departure of oxygen stoichiometry gives a limitation as observed in TiO_2 rutile grain boundary. If one attaches the more important weight to the bulk resistivity without need of permittivity larger than 15,000, several samples appear convenient. On the other hand, much higher permittivity can be reached like in CCTO@TiO_2 but at the expense of dielectric losses. Thermal post-treatment under various oxidizing or reducing atmosphere have to be developed to solve the problem of dielectric losses like in the example of CCTO@Al_2O_3 post-annealed at 550°C under oxygen.

Acknowledgements

This work was supported by Conseil régional Centre-Val de Loire (France).

References

[1] Chiou, B.S., Lin, S.T., Duh, J.G., Chang, P.H. Equivalent circuit model in Grain-Boundary Barrier Layer capacitance. *J. Am. Ceramic Soc.* **72** (1989) 1967-1975.

[2] Subramanian, M.A., Li. D., Duan, N., Reisner, B.A., Sleight, A.W. High dielectric constant in $ACu_3Ti_4O_{12}$ and $ACu_3Ti_3FeO_{12}$ phases. *J. Solid State Chem.* **151** (2000) 23-5.

[3] Ramirez, A.P., *et al* Giant dielectric constant response in a copper-titanate. *Solid State Commun.* **115** (2000) 217-220.

[4] Homes, C.C., Vogt, T., Shapiro, S.M., Wakimoto, S., Ramirez, A.P. Optical reponse of of high-dielectric-constant perovskite-related oxide. *Science* **293** (2001) 673-676.

[5] Sinclair, D.C., Adams, T.B., Morrison, F.D., West, A.R. $CaCu_3Ti_4O_{12}$: one-step internal barrier layer capacitor. *Appl. Phys. Lett.* **80** (2002) 2153-5.

[6] Adams, T.B., Sinclair, D.C., West, A.R. Influence of processing conditions on the electrical properties of $CaCu_3Ti_4O_{12}$ ceramics. *J. Am. Ceram. Soc.* **89** (2006) 3129-3135.

[7] Schmitt, R., Sinclair, D.C. $CaCu_3Ti_4O_{12}$ (CCTO) ceramics for capacitor applications. In *Capacitors: theory of operation, behaviour and safety regulations*, K. N. Muller, Ed., Nova Science Publishers Inc., New York – 2013

[8] Liu, L., Fan, H., Fang, P., Jin, L. Electrical heterogeneity in $CaCu_3Ti_4O_{12}$ ceramics fabricated by sol–gel method. *Solid State Communications 142 (2007) 573–576.*

[9] Liu, L., Fan, H., Fang, P., Chen, X. Sol–gel derived CaCu3Ti4O12 ceramics: Synthesis, characterization and electrical properties. *Materials Research Bulletin 43 (2008) 1800–1807.*

[10] Ahmadipour, M., Ain, M.F., Ahmad, Z.A. A short review on copper calcium titanate (CCTO) electroceramics: synthesis, dielectric properties, film deposition and sensing application. *Nano-Micro Lett. 8 (*2016) *291–311.*

[11] Liu, L., Fan, H., Chen, X., Fang, P., Electrical properties and microstructural characteristics of nonstoichiometric $CaCu_{3x}Ti_4O_{12}$ ceramics. *Journal of Alloys and Compounds 469 (2009) 529–534.*

[12] Mauczok, R., Wernicke, R. Ceramic boundary-layer capacitors. *Philips Tech. Rev.* **41** (1983) 338-346.

[13] Marchin, L., Guillemet-Fritsch, S., Durand, B., Levchenko, A.A., Navrotsky, A., Lebey, T. Grain growth-controlled giant permittivity in soft chemistry $CaCu_3Ti_4O_{12}$ ceramics. *J. Am. Ceram. Soc.* **91** (2008) 485-9.

[14] De Almeida-Didry, S., Autret, C., Honstettre, C., Lucas, A., Zaghrioui, M., Pacreau, F., Gervais, F. Central role of TiO_2 anatase grain boundaries on resistivity of $CaCu_3Ti_4O_{12}$-based materials probed by Raman spectroscopy. *Solid State Science*, **61** (2016) 102-105.

[15] Peng, H.P., Liang, R.P., Qiu, J.D. Facile synthesis of Fe_3O_4@Al_2O_3 core-shell nanoparticles and their application to the highly specific capture of heme proteins for direct electrochemistry. *Biosensors & Bioelectronics* **26** (2011) 3005-3011 – Peng, Y.K., *et al* A new and facile method to prepare uniform hollow MnO/functionalized mSiO_2 core/shell nanocomposites - 2011 *ACS Nano* doi.org/10.1021/nn200928r

[16] De Almeida-Didry, S., Autret, C., Lucas, A., Honstettre, C., Pacreau, F., Gervais, F. Leading role of grain boundaries in colossal permittivity of doped and undoped CCTO. *J. Eur. Ceram. Soc.* **34** (2014) 3649-3654.

[17] Liu, L. Shi, D., Zheng, S., Huang, Y., Wu, S., Li, Y., Fang, L., Hu, C. Polaron relaxation and non-ohmic behavior in $CaCu_3Ti_4O_{12}$ ceramics with different cooling methods. *Materials Chemistry and Physics 139 (2013) 844-850.*

[18] Liu, L., Fang, L., Huang, Y., Li, Y., Shi, D., Zheng, S., Wu, S., Hu, C. Dielectric and nonlinear current-voltage charactéristics of rare-earth doped $CaCu_3Ti_4O_{12}$ ceramics J. applied Phys. 110 (2011) 094101

[19] De Almeida-Didry, S., Autret, C., Honstettre, C., Lucas, A., Pacreau, F., Gervais, F. Capacitance scaling of grain boundaries with colossal permittivity of $CaCu_3Ti_4O_{12}$-based materials Solid State Sciences 42 (2015) 25-29

[20] Liu, L., Fan, H., Wand, L., Chen, X., Fang, P. DC-bias-field-induced dielectric relaxation and ac conduction in CaCu3Ti4O12 ceramics J. Philosophical Magazine 88 (2008) 537-545

[21] Gervais, F., Piriou, B., 1974. Temperature dependence of transverse- and longitudinal-optic modes in TiO_2 rutile. *Phys. Rev.* B **10**, 1642–1654.

[22] Baumard, J.F., Gervais, F. Plasmon and polar optical phonon in reduced rutile TiO_{2-x}. Phys. Rev. B **15** (1977) 2316-27.

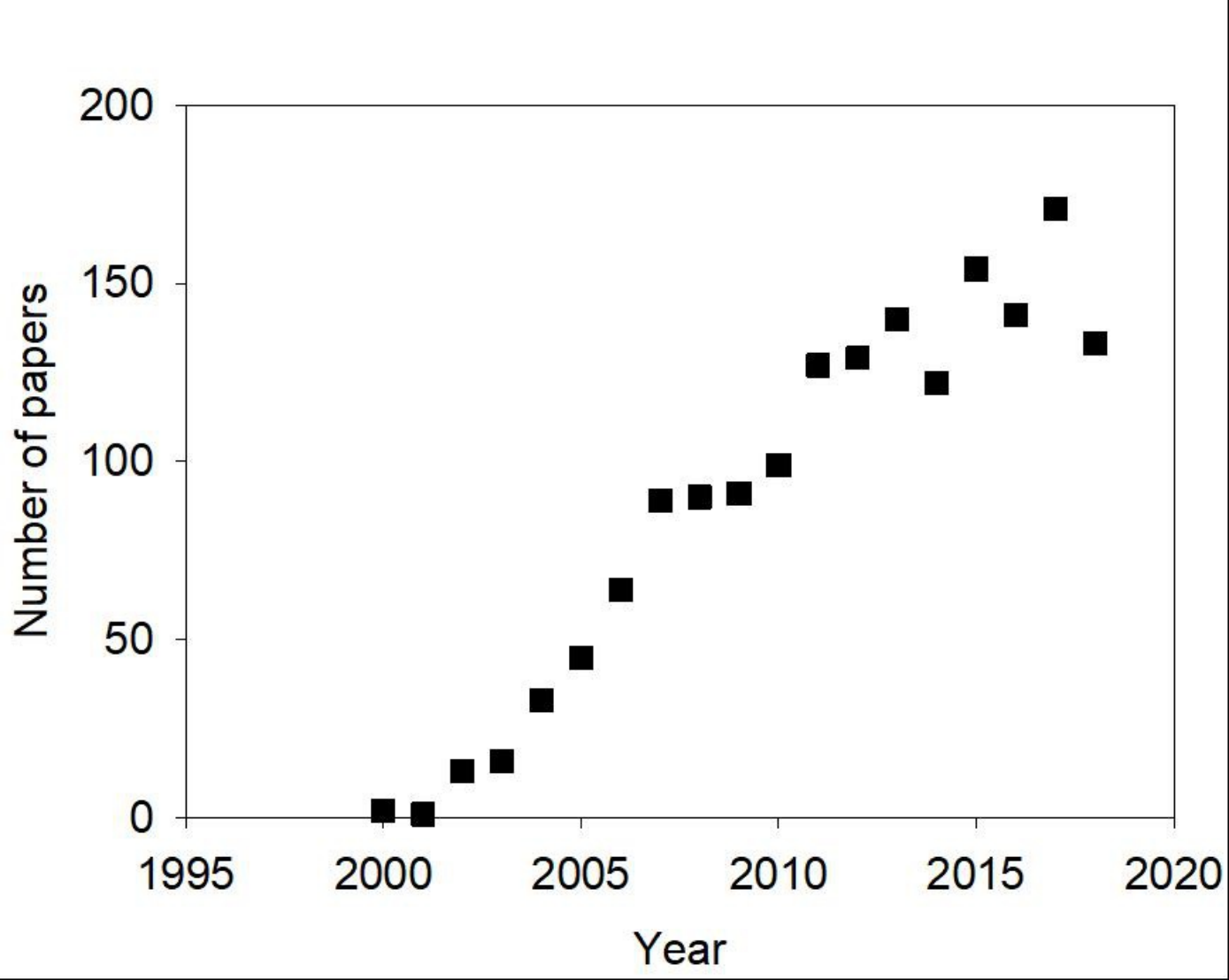
200
150
100
50
0
Number of papers
1995
2000
2005
2010
2015
2020
Year

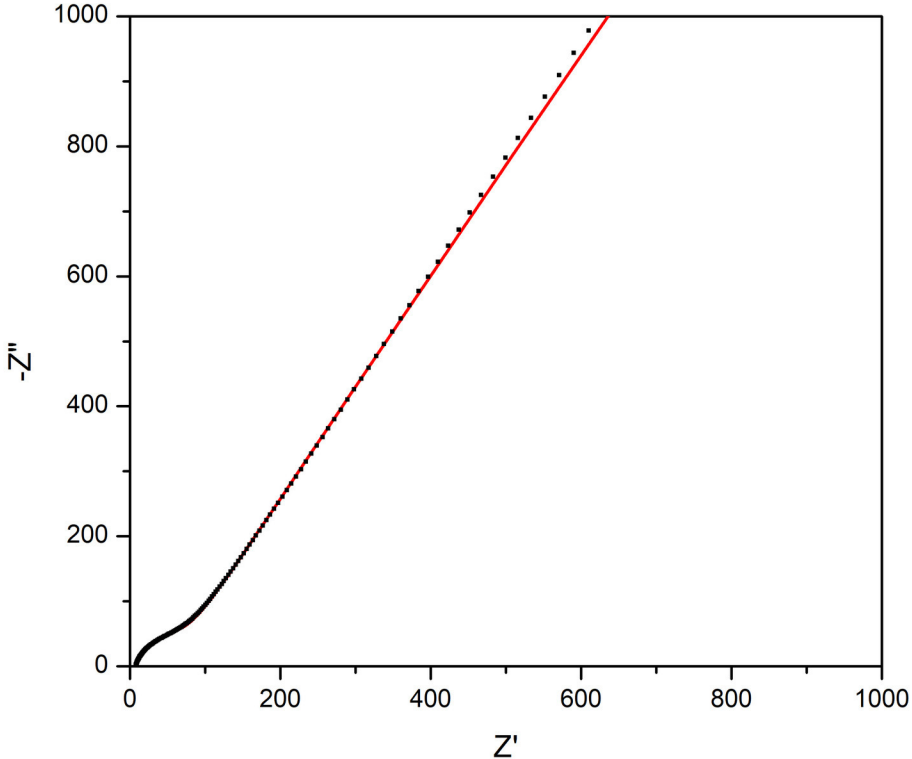
1000
800
600
400
200
0
-Z''
0
200
400
600
800
1000
Z'

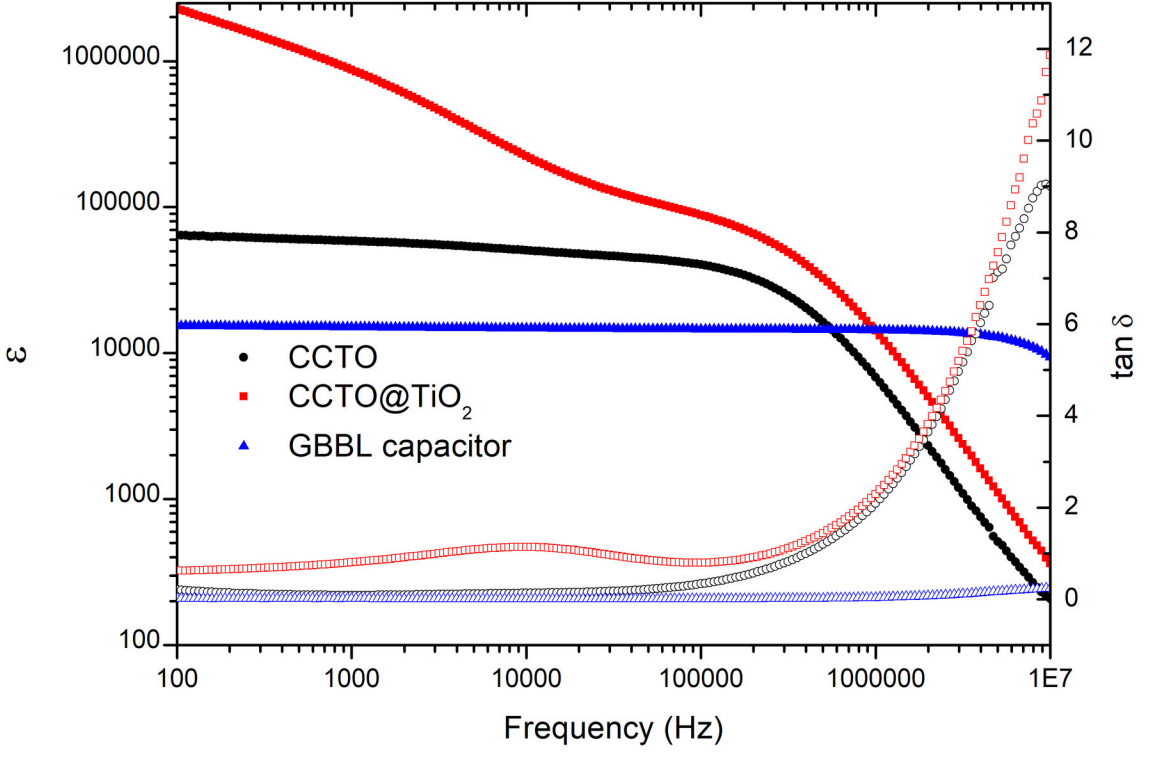
1000000
100000
10000
1000
100
ε
CCTO
CCTO@TiO2
GBBL capacitor
12
10
8
6
4
2
0
tan δ
100
1000
10000
100000
1000000
1E7
Frequency (Hz)

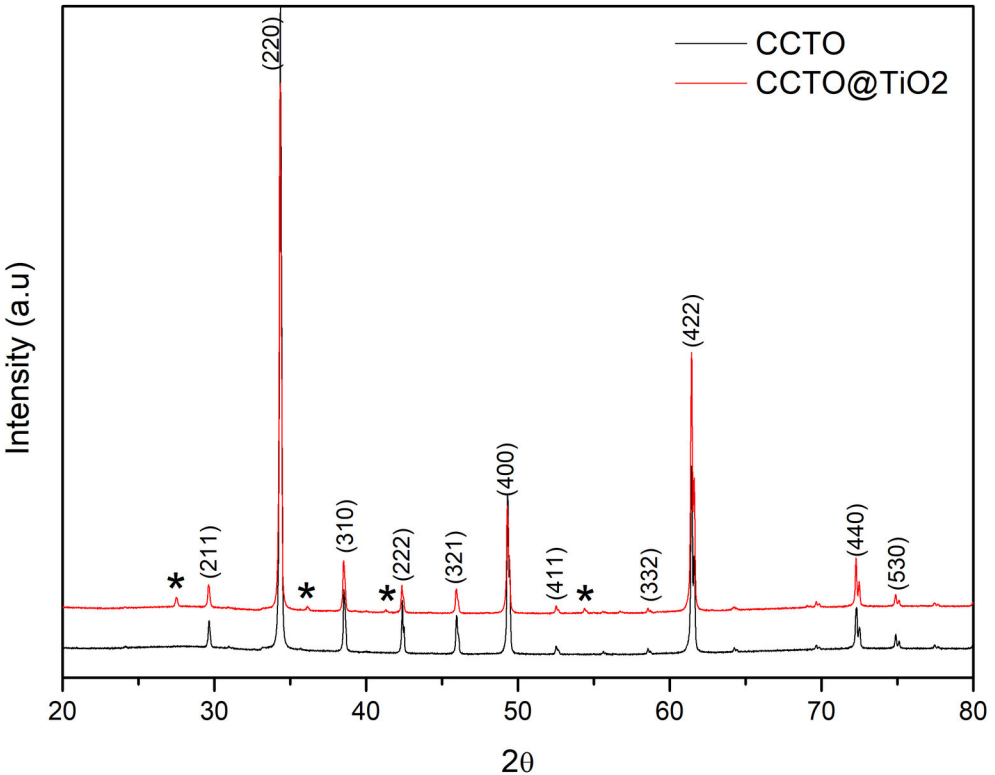
CCTO
CCTO@TiO2
Intensity (a.u)
2θ
(220)
(211)
(310)
(222)
(321)
(400)
(411)
(332)
(422)
(440)
(530)
*
20
30
40
50
60
70
80

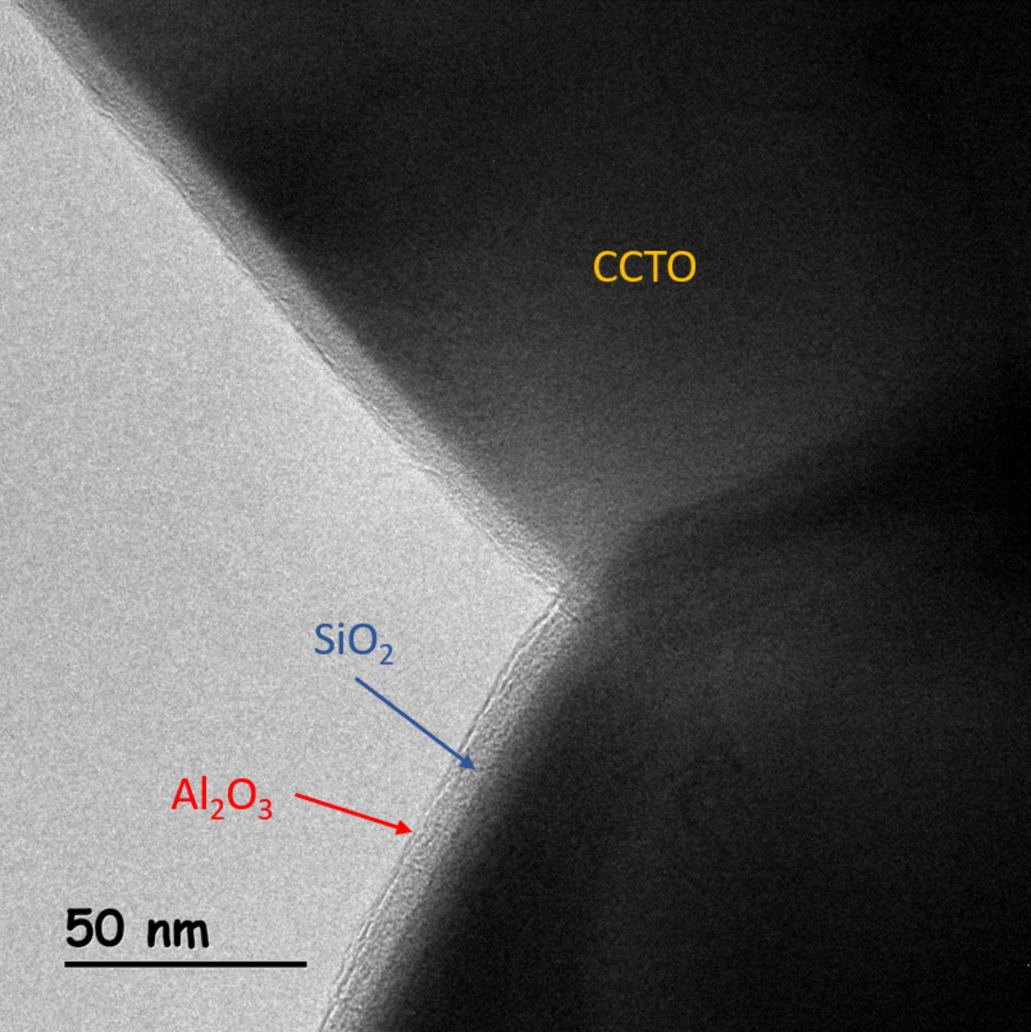
CCTO
SiO_2
Al_2O_3
50 nm

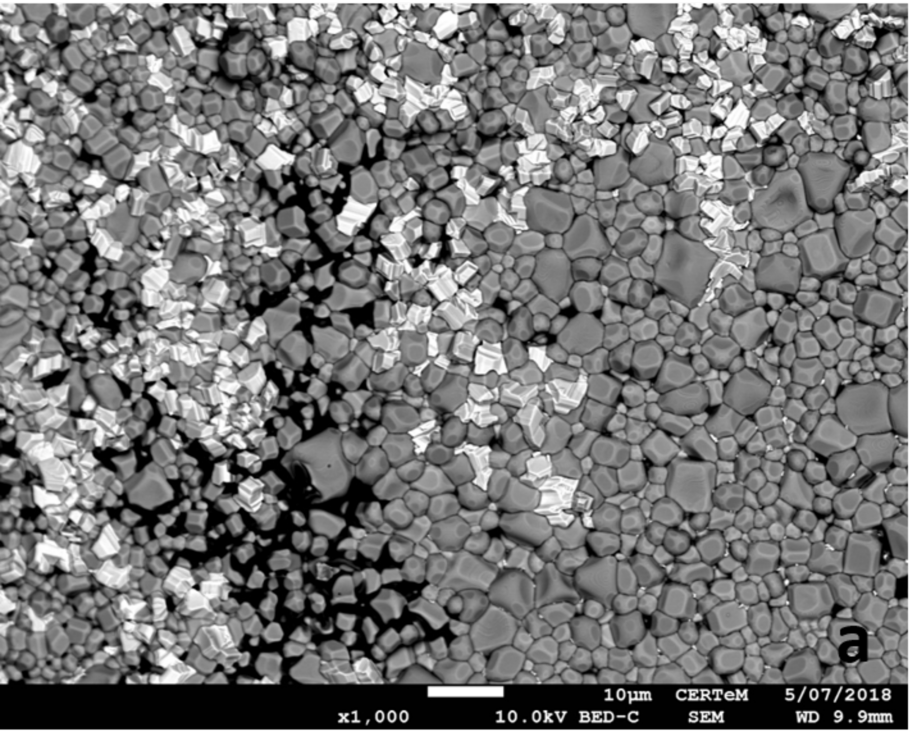

Image EDS en superposition 1

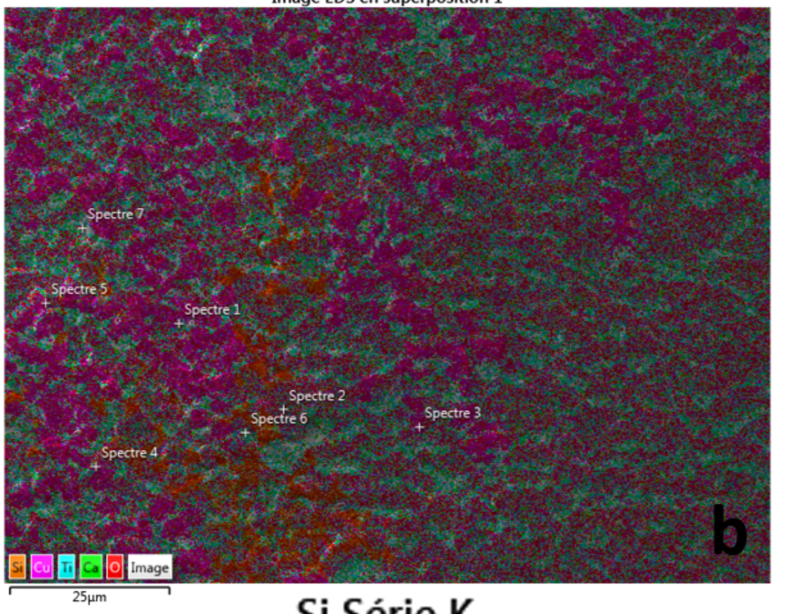

Si Série K

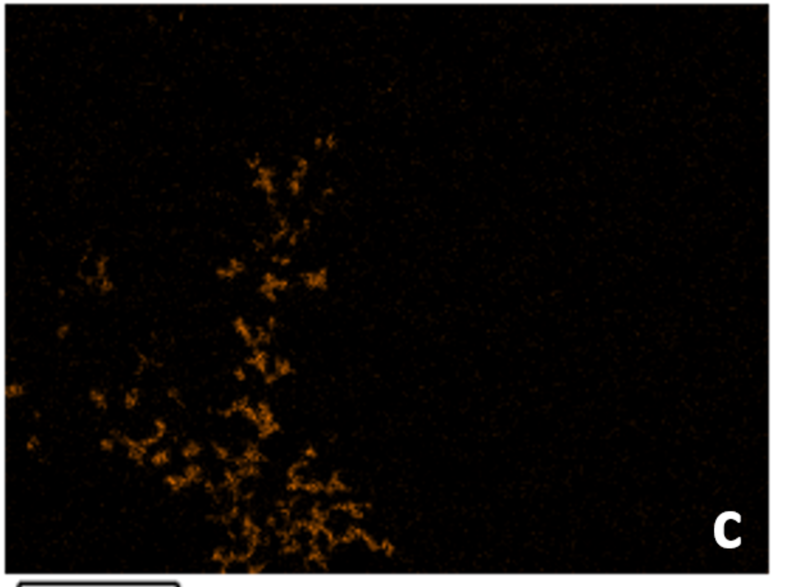

	ε at 1 kHz	tan(δ) at 1 kHz	Bulk resistivity (Ω.cm)	C_{gb} ($F.cm^{-1}$)	R_{gb} (Ω.cm)
Undoped CCTO-24 h	62,000	0.05	$1.3\ 10^{7}$	$4.5\ 10^{-7}$	$8.5\ 10^{6}$
CCTO@Al_2O_3	91,000	0.06	$1.5\ 10^{7}$	$5.5\ 10^{-8}$	$1.2\ 10^{6}$
CCTO@Al_2O_3+PEG	130,000	0.07	$3.9\ 10^{7}$	$4.2\ 10^{-8}$	10^{8}
CCTO@Al_2O_3+PVP	78,600	0.08	$1.9\ 10^{8}$	$2.25\ 10^{-8}$	$1.8\ 10^{7}$
CCTO@Al_2O_3+O_2 500°C	17,000	0.09	$1.9\ 10^{9}$	$9\ 10^{-9}$	$4\ 10^{7}$
CCTO@SiO_2	38,000	0.096	$1.1\ 10^{7}$	$3.5\ 10^{-8}$	$9\ 10^{5}$
CCTO@SiO_2@Al_2O_3	16,700	0.098	$5\ 10^{9}$	$2.9\ 10^{-9}$	$3\ 10^{7}$
CCTO@TiO_2	870,000	0.8	$2\ 10^{6}$	$1.06\ 10^{-5}$	$8.8\ 10^{4}$
CCTO@SiO_2@TiO_2	4,700	0.17	$5.2\ 10^{8}$	$1.5\ 10^{-8}$	$1.5\ 10^{6}$
Johanson GBBL	15,000	0.01	10^{10}	10^{-10}	10^{10}

Table 1 – A comparison of properties of undoped CCTO, core-shell samples and commercial GBBL capacitor.